

Magnetic resonance studies of Mg-doped GaN epitaxial layers grown by organometallic chemical vapor deposition

E. R. Glaser, W. E. Carlos, G. C. B. Braga,* J. A. Freitas, Jr., W. J. Moore,† B. V. Shanabrook, R. L. Henry, A. E. Wickenden,‡ and D. D. Koleske§
Naval Research Laboratory, Washington, D.C. 20375-5347

H. Obloh

Fraunhofer-Institut für Angewandte Festkörperphysik, D-79108 Freiburg, Germany

P. Kozodoy,|| S. P. DenBaars, and U. K. Mishra

Department of Electrical and Computer Engineering, University of California, Santa Barbara, California 93016
 (Received 6 July 2001; revised manuscript received 31 October 2001; published 5 February 2002)

Electron paramagnetic resonance (EPR) and optically detected magnetic resonance (ODMR) experiments have been performed on a set of GaN epitaxial layers doped with Mg from 2.5×10^{18} to $5.0 \times 10^{19} \text{ cm}^{-3}$. The samples were also characterized by secondary-ion-mass spectroscopy (SIMS), temperature-dependent Hall effect, and low-temperature photoluminescence (PL) measurements. EPR at 9 GHz on the conductive films reveals a single line with $g_{\parallel} \sim 2.1$ and $g_{\perp} \sim 2$ and is assigned to shallow Mg acceptors based on the similarity of the spin density with that found for the number of uncompensated Mg shallow acceptors from Hall effect and the total Mg concentration by SIMS. PL bands of different character are observed from these layers, including shallow-donor–shallow-acceptor recombination at 3.27 eV from the lowest doped sample and, in most cases, broad emission bands with peak energy between 2.8 and 3.2 eV from the more heavily doped films. In addition, several of the films exhibit a weak, broad emission band between 1.4 and 1.9 eV. ODMR at 24 GHz on the “blue” PL bands reveals two dominant features. The first is characterized by $g_{\parallel}, g_{\perp} \sim 1.95\text{--}1.96$ and is assigned to shallow effective-mass donors. The second line is described by similar g tensors as found by the EPR experiments and, thus, is also attributed to shallow Mg acceptors. Although several groups have related the 2.8 eV PL in heavily Mg-doped GaN with the formation of deep donors, no clear evidence was found from the ODMR on this emission for such centers. However, based on the near-midgap PL energy and the observation of the feature assigned to shallow Mg acceptors, the strongest case from magnetic resonance for the existence of deep donors in these films is the isotropic ODMR signal with $g = 2.003$ found on emission < 1.9 eV. Possible recombination mechanisms to account for the ODMR on these “blue” and near-IR PL bands are discussed.

DOI: 10.1103/PhysRevB.65.085312

PACS number(s): 78.66.Fd, 71.55.Eq, 76.30.-v, 76.70.Hb

I. INTRODUCTION

Mg is the most widely employed dopant for p -type conduction in GaN. In addition to the rather large thermal ionization energy (~ 180 meV), there appear to be other factors (such as self-compensation and/or complexing, clustering, etc) that limit typical room-temperature hole densities to the range of low- to mid- 10^{17} cm^{-3} in GaN epitaxial layers grown by organometallic chemical vapor deposition (OMCVD).¹ However, larger hole concentrations are desired to improve blue-green laser performance and to create high-performance heterojunction bipolar transistors (HBTs). Other potential p -type dopants have been tried but with little overall success. For example, Zn, Cd, and Hg are even deeper than Mg. Be is a promising candidate for enhanced p -type conductivity in GaN based on the binding energy ($E_a \sim 100$ meV) deduced from photoluminescence (PL) studies; however, the existence of self-compensating (donor) centers and/or Be-related deep acceptor complexes renders such material highly resistive in most reported cases.²

In order to provide more details on the nature of the Mg acceptors and Mg-related or -induced compensating centers, comprehensive electron paramagnetic resonance (EPR) and

optically detected magnetic resonance (ODMR) experiments have been performed on a set of GaN epitaxial layers grown by OMCVD from three laboratories. The films were doped with Mg from 2.5×10^{18} to $5 \times 10^{19} \text{ cm}^{-3}$ as measured by secondary-ion-mass spectroscopy (SIMS). In addition we have attempted to correlate the magnetic resonance results with those obtained from SIMS, temperature-dependent Hall effect, and low-temperature PL studies of the same samples or nearby pieces of the wafers in order to form a self-consistent picture.

In general, EPR provides information on the ground state and microscopic origin of defects through the Zeeman splittings (g factors) and, in best cases, resolved hyperfine structure. In addition, the number of uncompensated (neutral) centers can be determined from the integrated intensity of the signal and an appropriate standard. ODMR, though not quantitative, combines the attributes of EPR with the sensitivity and selectivity of PL (Ref. 3). The technique yields information on the magnetic properties of the optically excited donor (electron) and acceptor (hole) states that participate directly (or, in some cases, indirectly) in the recombination processes.

The present work expands on a preliminary ODMR inves-

tigation of metal-organic chemical-vapor deposition-(MOCVD) grown GaN as a function of Mg doping level.⁴ The main results are as follows. First, EPR reveals a strong signal from p -type conductive layers with $g_{\parallel} \sim 2.1$ and $g_{\perp} \sim 2$. This resonance is assigned to uncompensated shallow Mg acceptors based on the similarity of the spin density with that found for the number of uncompensated shallow Mg acceptors as determined by Hall effect and the total Mg concentration by SIMS. Second, PL bands of different character are found from these films, including strong shallow-donor—shallow-acceptor (SD-SA) recombination with zero-phonon line (ZPL) at 3.27 eV from the lowest doped sample and, with one exception, broad emission bands with peak energy between 2.8 and 3.2 eV from the more heavily doped films. In addition, most of these films exhibit a weak, broad emission band with peak energy near 1.7 eV. Third, Hall effect measurements reveal $\sim 5\%$ – 10% compensation ($\sim 10^{18} \text{ cm}^{-3}$ shallow and/or deep donors) of the activated acceptors with a Mg ionization energy of 185 meV. Fourth, although several groups^{5–12} have attributed some fraction of these compensating centers and the occurrence of the broad 2.8 eV “blue” PL band with Mg-doping-induced deep donors, no CLEAR evidence was found from ODMR on this emission for such centers. However, evidence for deep donors was revealed from ODMR on the broad PL less than 1.9 eV. Finally, ODMR reveals similar acceptorlike resonances on BOTH the “blue” and near-infrared (~ 1.7 eV) PL bands as found by EPR, including that associated with shallow Mg acceptors that participate in the 3.27-eV SD-SA recombination.

The paper is divided into five sections. Section I is the introduction. The set of samples investigated in this work is described in Sec. II. In addition, a few details of the PL and magnetic resonance techniques are also given. The main results from the SIMS, Hall effect, PL, EPR, and ODMR experiments are presented in Sec. III. A discussion of the results is provided in Sec. IV, including models proposed for the recombination processes observed in these films. In addition, we place this work in the context of other recent experimental and theoretical efforts undertaken to address the behavior of Mg acceptors in GaN. Overall conclusions are given in Sec. V.

II. EXPERIMENTAL DETAILS

The experiments were performed on five GaN epitaxial layers (referred to as Nos. 1–5) from three laboratories grown on a -plane and c -plane Al_2O_3 substrates by MOCVD. The 1.0–2.5- μm -thick films were doped with Mg and subsequently annealed in an inert atmosphere near 1000 °C to activate the Mg acceptors as typically required for the CVD growth technique. Additional details of the growth are described elsewhere.^{6,13,14}

Secondary-ion-mass spectroscopy (SIMS) was employed to determine the total Mg concentration in the films. In addition, SIMS depth profiles of Si, H, O, and C were obtained in select films. The transport properties of the Mg-doped GaN layers were extracted from either Hall effect or two-point probe measurements. In some cases (sample Nos. 3 and

TABLE I. Mg-doped GaN epitaxial layers investigated in this work (NRL≡Naval Research Laboratory, FB≡IAF Freiburg, UCSB≡University of California at Santa Barbara).

Sample designation	Thickness (μm)	[Mg] ^a (cm^{-3})	Carrier concentration (300 K) (cm^{-3})
No. 1 (NRL #980804)	1.5	2.5×10^{18}	Highly resistive
No. 2 (FB #2947)	2.5	1.4×10^{19}	Highly resistive
No. 3 (NRL #980805)	1.5	$2\text{--}5 \times 10^{19}$	$p \sim 9 \times 10^{16}$
No. 4 (NRL #990607)	1.6	$2\text{--}4 \times 10^{19}$	$p \sim 1.7 \times 10^{17}$
No. 5 (UCSB #990401PB)	~ 1	$3\text{--}4 \times 10^{19}$	$p \sim 2.7 \times 10^{17}$

^aDetermined from SIMS depth profiles.

4) variable-temperature Hall effect (80–600 K) experiments were carried out to obtain more detailed information such as the dopant ionization energy and degree of compensation in the films. The layer thickness, Mg doping levels, and room-temperature carrier concentrations for the five samples are summarized in Table I.

The PL at 1.6 K was excited by the 351-nm line of an Ar^+ laser at a power density of $\sim 1 \text{ W/cm}^2$. The emission between 1.25 and 3.5 eV was analyzed by a 0.22-m double-grating spectrometer and detected by either a Si photodiode or a UV-enhanced GaAs photomultiplier tube. The spectra were corrected for the system response by normalization to the throughput of a broadband calibration lamp.

The EPR experiments were done at 4.2 K in a Bruker 300 ESP X-band (9.5 GHz) spectrometer configured with a liquid-helium flow cryostat for temperature control. Angular rotation studies were performed in the (1120) plane to obtain symmetry information. A few milligrams of P-doped Si powder embedded in polyethylene was used as a standard to determine the spin density associated with the signals observed from the Mg-doped GaN layers.

The ODMR was performed at 1.6 K in a 24-GHz spectrometer with the samples placed in the tail section of an optical cryostat. The ODMR signal corresponds to the change in the intensity of the PL which was coherent with the on-off amplitude modulation ($\sim 77 \text{ Hz}$ to 3 kHz) of 50 mW of microwave power under a swept dc magnetic field. Two detection schemes were employed. First, emission bands were separately analyzed with either visible bandpass or near-infrared cutoff filters placed in front of the Si photodiode. Second, the ODMR was also obtained using the same spectrometer-GaAs detector combination described above in order to study the character of the magnetic resonance at several energy positions.

III. RESULTS

A. SIMS

In addition to the determination of the Mg dopant levels in these films (see Table I), SIMS depth profiles of Si, C, O, and H (common residual impurities in CVD-grown GaN) were also obtained¹⁵ for a subset of samples after the post-growth anneals. Si and O, in particular, can act as donors to compensate the electrically active Mg acceptors. In addition

TABLE II. Concentrations of residual impurities in select samples determined from SIMS depth profiles.

Sample designation	Si (cm^{-3})	O (cm^{-3})	C (cm^{-3})	H (cm^{-3})
No. 3 (NRL #980805)	$(6 \times 10^{17})^a$	1×10^{17}	1×10^{17}	$1-2 \times 10^{19}$
No. 4 (NRL #990607)	1.3×10^{17}	1×10^{17}	1.4×10^{17}	4×10^{18}
No. 5 (UCSB #990401PB)	$2-3 \times 10^{17}$	1×10^{17}	2×10^{17}	

^aEstimated from SIMS of samples grown under similar conditions.

to its role as a passivating species of Mg prior to the high-temperature anneal treatments, H has been suggested recently as another source of shallow donors in GaN (Ref. 10). The SIMS results for samples Nos. 3–5 are summarized in Table II. Two features are highlighted based on this data set and other Mg-doped GaN layers grown at NRL under similar conditions (Mg doping level, growth pressure, etc.). First, the residual concentrations of Si, O, and C are comparable ($\sim 1-3 \times 10^{17} \text{ cm}^{-3}$). Second, the H level is still rather high (mid- $10^{18}-10^{19} \text{ cm}^{-3}$) even after the post-growth anneals.

B. Electrical properties

Two-point probe measurements indicated that sample Nos. 1 and 2 were highly resistive while samples Nos. 3–5 (more heavily doped films) were found to be conductive. Detailed temperature-dependent Hall effect studies were performed on sample Nos. 3 and 4 in the usual van der Pauw cloverleaf geometry with indium contacts. As an example, the hole concentration plotted as a function of the inverse temperature for sample No. 4 is shown in Fig. 1. As observed by other groups,¹⁴ the increase in hole concentration for $T < 125 \text{ K}$ is attributed to the onset of hopping or impurity-band conduction. The concentrations of Mg acceptors (N_A), the ionization energy (E_a), and the compensating donors

(N_D) were determined from a fit to the high-temperature data using the charge-balance equation for a single carrier (the Hall scattering factor r_H was assumed to be 1). The best fit (solid line in Fig. 1) yielded an active Mg concentration of $4 \times 10^{19} \text{ cm}^{-3}$ with E_a of 185 meV and $1.8 \times 10^{18} \text{ cm}^{-3}$ compensating donors ($N_D/N_A \sim 5\%$). An active Mg concentration of $1.8 \times 10^{19} \text{ cm}^{-3}$ with E_a of 185 meV and $\sim 10\%$ compensation were found for sample No. 3. We note that the Mg concentrations extracted from the variable-temperature Hall measurements are similar, within the respective errors, to the total Mg levels revealed by SIMS. Finally, the room-temperature mobilities of sample Nos. 3–5 were $\sim 15-22 \text{ cm}^2/(\text{V sec})$, quite typical for Mg-doped GaN.¹⁴

C. PL

The dominant PL bands observed at 1.6 K under an excitation power density (P_{exc}) of $\sim 1 \text{ W/cm}^2$ are shown in Fig. 2. Recombination bands of different character are found (commonly referred to as the “blue” emission bands). With the exception of sample No. 5, similar PL results as a function of the total Mg concentration are generally observed for CVD-grown GaN (Refs. 5, 6, 8, and 16–18). We note that the structure on the broad PL from sample Nos. 2–4 is due to

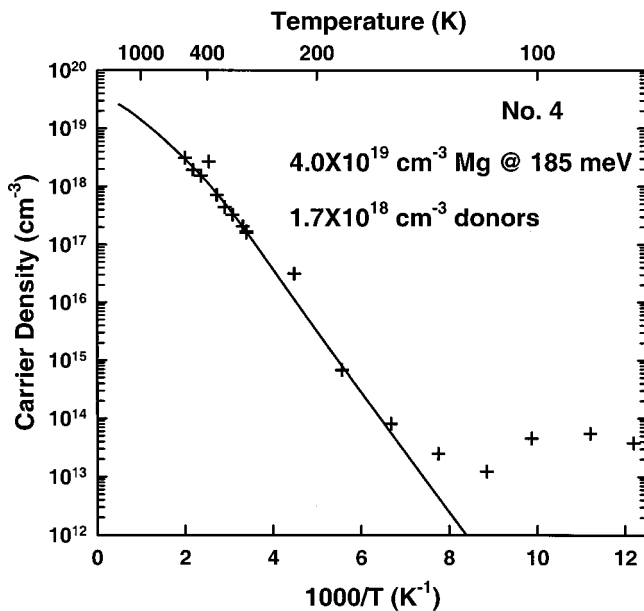


FIG. 1. Temperature-dependent hole concentration for Mg-doped GaN sample No. 4. The solid line is a fit to the data for $T \geq 125 \text{ K}$ as described in the text.

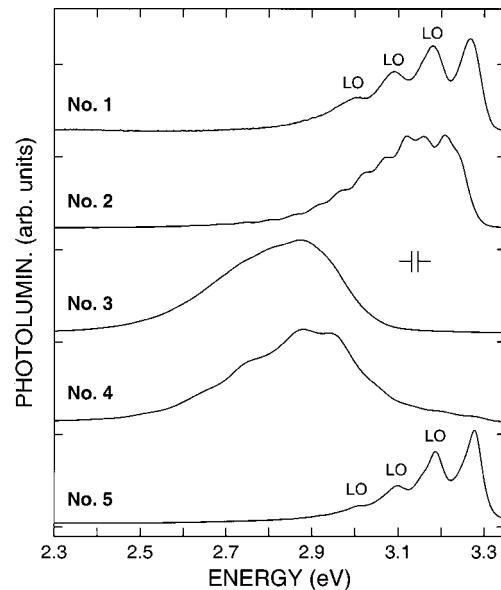


FIG. 2. Photoluminescence obtained at 1.6 K in the “blue” spectral region from five Mg-doped GaN layers (LO=longitudinal optical phonon replica).

Fabry-Perot interference fringes. Also, more detailed optical studies of some of these samples will be reported elsewhere.¹⁹

Sample No. 1 exhibits strong recombination at 3.27 eV (zero-phonon line) and a series of LO-phonon replicas at lower energies. Excitation power studies reveal a monotonic shift of this peak to lower energy by ~ 15 meV with P_{exc} reduced by a factor of 1000. Following previous work,¹⁶ this emission is attributed to a recombination between shallow donors and shallow Mg acceptors ($E_a \sim 230$ meV). Likely candidates for the shallow donors are Si and/or O with binding energies (E_d) of 30.2 and 33.2 meV, respectively.²⁰

The dominant emission observed from sample No. 2 is broad with peak energy at ~ 3.15 eV. This band is also characterized by its asymmetric line shape. Similar emission has been observed by Reshchikov *et al.*⁵ Based on the evolution of this PL with increasing P_{exc} from a broad, structureless band at ~ 3.2 eV to a sharper peak at 3.27 eV (+LO-phonon replicas), this group assigned the emission to recombination between shallow donors and shallow acceptors in the presence of large potential fluctuations. As also reported for other semiconductor systems such as highly compensated and doped GaAs (Ref. 21) and ZnSe (Refs. 22 and 23), these fluctuations arise from a random distribution of positively and negatively charged impurities.²⁴ However, no significant change was found in the character of the emission from sample No. 2 with P_{exc} varied between 1 W/cm² and 1 kW/cm² (Ref. 25).

The strongest emission observed from sample Nos. 3 and 4 is also broad with peak energy near 2.8 eV. The PL is also slightly asymmetric. Most notably, the bands shift to higher energy by 100–150 meV with increasing excitation power. Similar emission has been reported by many groups for GaN doped with $\text{Mg} \geq 2-3 \times 10^{19}$ cm⁻³. Its origin has been the subject of much debate. In particular, several workers have proposed that the band arises from recombination between Mg-related deep donors with $E_d \sim 0.3-0.5$ eV and shallow Mg acceptors.⁵⁻¹²

Instead of the broad “blue” emission band near 2.8 eV often observed from GaN at such high Mg doping levels, sample No. 5 exhibits PL at 3.28 eV and a series of LO-phonon replicas. We note that the ZPL is at a slightly higher-energy position and is sharper (including the LO-phonon replicas) than observed for the emission from sample No. 1. However, in contrast to sample No. 1, no shift was found for P_{exc} varied between 0.001 and 1 W/cm².

In addition to the “blue” emission bands, the samples exhibit weak recombination between 1.4 and 1.9 eV. Part of this broad emission arises from the underlying sapphire substrates that are preferentially excited by the “blue” PL bands.²⁶ A rough estimate of ~ 1.65 eV was found for the peak of the near-IR emission from the Mg-doped GaN layers after subtraction of the PL obtained from a piece of a-plane sapphire. Similar broad emission (referred to as the “red” PL band) has been reported recently for Mg-doped GaN grown by CVD, molecular beam epitaxy, and high-pressure-high-temperature synthesis,^{27,28} for CVD-grown GaN codoped with Mg and Si (Ref. 6), and for undoped (*n*-type) GaN grown by HVPE.²⁶

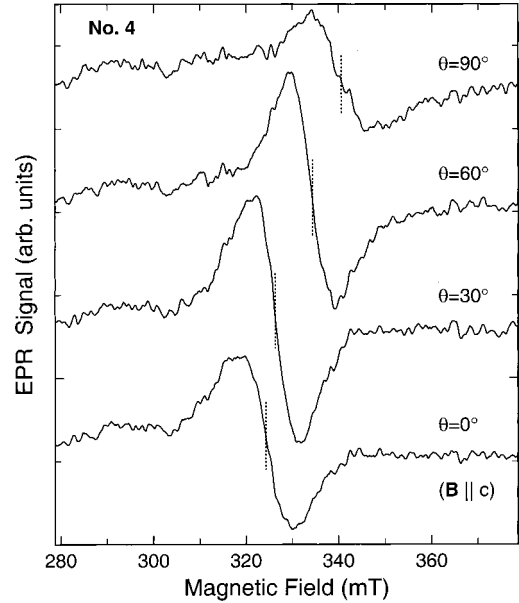


FIG. 3. EPR spectra at 9.5 GHz for *p*-type sample No. 4 as a function of the angle (θ) between \mathbf{B} and the *c* axis. Dotted lines indicate the resonance positions.

D. EPR

Representative EPR spectra obtained in the dark for *p*-type conductive sample No. 4 are shown in Fig. 3. A single, slightly anisotropic line is found with axial symmetry about the *c* axis. The extremal g values (g_{\parallel} and g_{\perp}) were determined from a fit to the expression $g(\theta) = (g_{\parallel}^2 \cos^2 \theta + g_{\perp}^2 \sin^2 \theta)^{1/2}$, where θ is the angle between the *c* axis and magnetic field. For this sample, $g_{\parallel} = 2.097 \pm 0.004$ and $g_{\perp} = 1.994 \pm 0.004$. A signal with similar resonance parameters ($g_{\parallel} = 2.0728 \pm 0.0015$ and $g_{\perp} = 1.9886 \pm 0.0015$) has been reported by another group from EPR of Mg-doped (conductive) GaN (Ref. 29). Two aspects of the linewidth are noted. First, the line is much broader ($\sim 12-15$ mT) than those typically found for EPR of shallow donors ($\sim 0.5-1$ mT) in undoped (*n*-type) and Si-doped GaN (Refs. 29–31). Second, a minimum in the linewidth is found with \mathbf{B} close to 30° from the *c* axis while the line is broadest with \mathbf{B} perpendicular to the *c* axis. Finally, the density of spins associated with this signal is estimated to be $\sim 4 \times 10^{19}$ cm⁻³ ($\pm 50\%$) from a comparison with the EPR of a P-doped Si standard.

Strong EPR lines were also observed from *p*-type sample Nos. 3 and 5 with g tensors and linewidths slightly different than those found for sample No. 4 (see Table III). As seen in sample No. 4, a similar narrowing of the linewidth by $\sim 20\%-30\%$ was also found for these samples with $\mathbf{B} \sim 30^\circ$ from the *c* axis. However, in contrast to the behavior observed for sample Nos. 3 and 4, the intensity of the EPR signal from sample No. 5 was found to diminish significantly for $\theta > 45^\circ$ such that it could no longer be detected above the background. This curious behavior has only been observed in the one sample and is somewhat reminiscent of the magnetic resonance found for $m_J = \pm 3/2$ shallow acceptor levels in other wurtzite (WZ) semiconductors where the intensity increases away from the *c* axis due to mixing with the

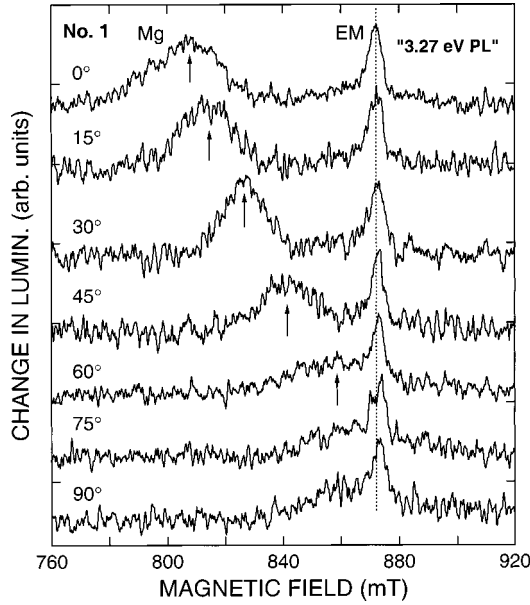


FIG. 4. ODMR spectra at 24 GHz detected on the 3.27-eV ZPL from sample No. 1 through the $\frac{1}{4}$ -m spectrometer. The dominant features are attributed to shallow donors (EM) and shallow (Mg) acceptors. The dotted line indicates the position of the EM resonance with $\mathbf{B} \parallel c$ ($\theta = 0^\circ$).

$m_j = \pm 1/2$ states.³² Here the trend is the opposite, but mixing of the $m_j = \pm 3/2$ and $\pm 1/2$ states may still play a role. However, until we have further data we leave the resolution of this issue for a later date. Finally, EPR was not detected above the background from sample Nos. 1 and 2, which transport measurements indicated were highly resistive.

E. ODMR

1. “Blue” PL bands

The ODMR spectra obtained on the 3.27-eV zero-phonon line from sample No. 1 through the 0.22-m spectrometer are shown in Fig. 4. Two luminescence-increasing signals are found. The first line (labeled EM) is sharp [full width at half maximum (FWHM) ~ 5 mT] with $g_{\parallel} = 1.952 \pm 0.001$ and $g_{\perp} = 1.949 \pm 0.001$. This feature is assigned to shallow, effective-mass (EM) donors based on previous magnetic resonance work.³³ The second signal (labeled Mg) is broad (FWHM ~ 30 mT) with $g_{\parallel} = 2.113 \pm 0.004$ and $g_{\perp} = 1.970 \pm 0.005$. This g tensor is similar to those found from EPR of p -type conductive GaN sample Nos. 3–5 (see Table III). In addition, similar to the trend observed for the EPR linewidths, this line narrows for $\mathbf{B} \sim 30^\circ$ from the c axis.

The ODMR found via collection of the entire 3.27–3.28 eV SD-SA and broad 2.8–3.2 eV PL bands (using bandpass filters) from the five samples with $\mathbf{B} \parallel c$ is shown in Fig. 5. The g values and linewidths are summarized in Table III. Except for the improvement in signal to noise, the spectrum obtained for sample No. 1 with this detection scheme is similar to that shown in Fig. 4. The ODMR on the 2.8–3.2 eV broad PL bands from the more heavily Mg-doped samples Nos. 2–4 also reveals two strong lines (i.e., $\Delta\text{PL}/\text{PL} \sim 1\%$).

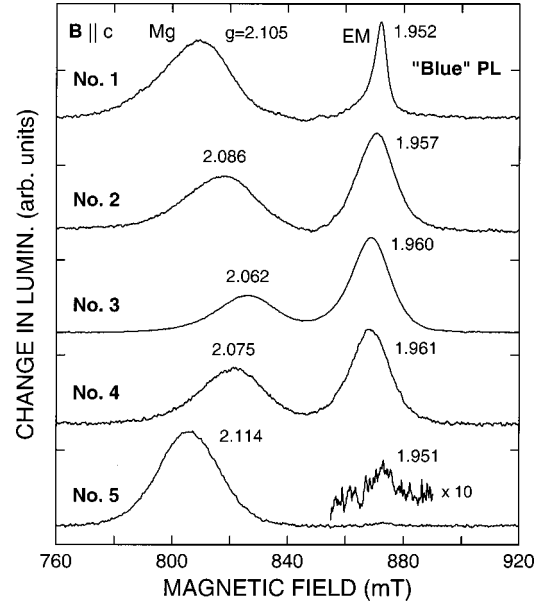


FIG. 5. ODMR found via detection of the entire “blue” PL bands from the five Mg-doped GaN layers with $\mathbf{B} \parallel c$.

Instead of the EM donor signal with $g \sim 1.95$, broader resonances (FWHM ~ 16 mT) with $g_{\parallel} \sim 1.960(2)$ and $g_{\perp} \sim 1.9555(2)$ are found. The second feature is characterized by $g_{\parallel} \sim 2.1$ and $g_{\perp} \sim 2.0$ with a FWHM of 26–28 mT, similar to the ODMR parameters obtained for the broad signal (Mg) on the SD-SA recombination from sample No. 1. A similar line is found on the 3.28 eV PL from sample No. 5. As seen in the EPR of this film, this resonance could not be observed above the noise for $\theta > 45^\circ$. We note that as observed for sample No. 1, the broad ODMR line from sample Nos. 2–5 narrowed by 30%–40% with $\theta \sim 30^\circ$. Finally, a weak feature with $g_{\parallel} = 1.951$ and FWHM of ~ 7 mT is also found on the emission from sample No. 5.

Detailed ODMR studies performed with the “blue” emission bands analyzed through the spectrometer revealed a shift to lower magnetic fields (hence, higher g values) of the broad resonance signals (Mg) with increasing detection energy. This behavior is shown for sample Nos. 1–3 in Fig. 6. For example, g_{\parallel} shifts monotonically from 2.058 to 2.074 with detection at several energies across the broad 2.8 eV PL band from sample No. 3.

2. $\text{PL} < 1.9$ eV

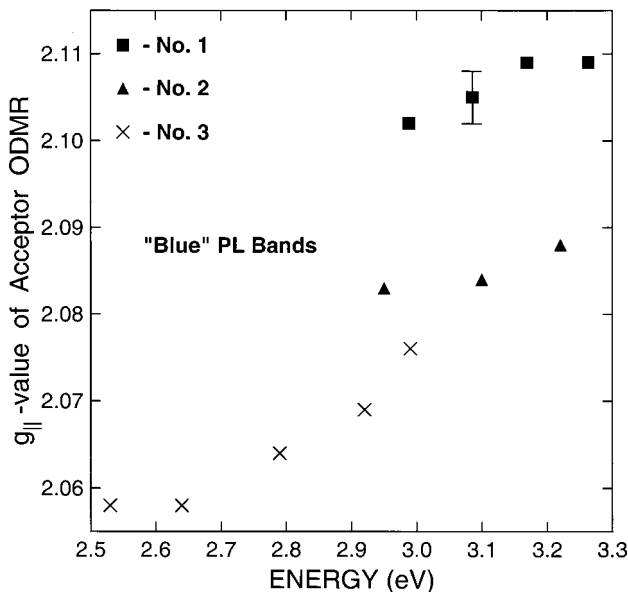
Representative ODMR obtained on emission less than 1.9 eV from sample Nos. 1–5 with $\mathbf{B} \parallel c$ are shown in Fig. 7. We note that ODMR was not observed on the $\text{PL} < 1.9$ eV from a piece of a -plane sapphire used in the growth of the NRL samples. Two luminescence-increasing signals are clearly observed for sample Nos. 1–4. The first is isotropic with $g = 2.003 \pm 0.002$ and a FWHM of ~ 15 –20 mT. Although the g values are similar, this feature is 3–4 times broader than the ODMR signal (referred to as MM1) reported recently on emission less than 2 eV from a variety of Mg-doped GaN samples.^{27,28} The second line is described by very similar g tensors ($g_{\parallel} \sim 2.1$, $g_{\perp} \sim 2.0$) and linewidths (~ 23 –25 mT) as

TABLE III. Magnetic resonance parameters from EPR and ODMR of Mg-doped GaN films. ND≡not detected.

Sample	[Mg] ^a (cm ⁻³)	EPR		ODMR on "blue" PL		ODMR on PL < 1.9 eV	
		Acceptor	Spin density (cm ⁻³)	Donor	Acceptor	Donor	Acceptor
No. 1 NRL #980804	2.5 × 10 ¹⁸	ND	—	$g_{\parallel} = 1.952(1)$ $g_{\perp} = 1.949(1)$ (FWHM ~ 5 mT)	$g_{\parallel} = 2.105(4)$ $g_{\perp} = 1.970(5)$ (FWHM ~ 28 mT)	$g_{\parallel}, g_{\perp} = 2.003(2)$ (FWHM ~ 19 mT)	$g_{\parallel} = 2.101(3)$ $g_{\perp} \sim 2$ (FWHM ~ 25 mT)
No. 2 (FB #2947)	1.4 × 10 ¹⁹	ND	—	$g_{\parallel} = 1.957(2)$ $g_{\perp} = 1.953(2)$ (FWHM ~ 16 mT)	$g_{\parallel} = 2.086(4)$ $g_{\perp} = 2.003(3)$ (FWHM ~ 28 mT)	$g_{\parallel}, g_{\perp} = 2.003(2)$ (FWHM ~ 15 mT)	$g_{\parallel} = 2.075(3)$ $g_{\perp} \sim 2$ (FWHM ~ 25 mT)
No. 3 (NRL #980805)	2–5 × 10 ¹⁹	$g_{\parallel} = 2.086(4)$, $g_{\perp} = 2.013(7)$ (FWHM ~ 14 mT) ^b	2 × 10 ¹⁹	$g_{\parallel} = 1.960(2)$ $g_{\perp} = 1.957(2)$ (FWHM ~ 16 mT)	$g_{\parallel} = 2.062(3)$ $g_{\perp} = 2.018(3)$ (FWHM ~ 26 mT)	$g_{\parallel}, g_{\perp} = 2.003(2)$ (FWHM ~ 20 mT)	$g_{\parallel} = 2.092(3)$ $g_{\perp} \sim 2$ (FWHM ~ 23 mT)
No. 4 (NRL #990607)	2–4 × 10 ¹⁹	$g_{\parallel} = 2.097(4)$, $g_{\perp} = 1.994(4)$ (FWHM ~ 12 mT)	4 × 10 ¹⁹	$g_{\parallel} = 1.961(2)$ $g_{\perp} = 1.955(2)$ (FWHM ~ 16 mT)	$g_{\parallel} = 2.075(3)$ $g_{\perp} = 2.015(3)$ (FWHM ~ 27 mT)	$g_{\parallel}, g_{\perp} = 2.003(2)$ (FWHM ~ 18 mT)	$g_{\parallel} = 2.104(3)$ $g_{\perp} \sim 2$ (FWHM ~ 25 mT)
No. 5 (UCSB #990401PB)	3–4 × 10 ¹⁹	$g_{\parallel} = 2.112(5)$ ($g_{\perp} \sim 2$) ^c (FWHM ~ 14 mT)	4 × 10 ¹⁹	$g_{\parallel} = 1.951(1)$ g_{\perp} (ND) (FWHM ~ 7 mT)	$g_{\parallel} = 2.114(3)$ g_{\perp} (ND) (FWHM ~ 25 mT)	ND	ND

^aDetermined from SIMS.^bLinewidths given for $\mathbf{B} \parallel c$.^cDetermined from fit of angular rotation data.

those for the broad ODMR signals (Mg) found on the respective "blue" PL bands from these four samples (see Table III). We note that this ODMR is different than that found on the "red" PL from HVPE-grown (undoped) GaN (Ref. 34). Finally, there is a suggestion for a weak luminescence-decreasing broad signal with $g_{\parallel} \sim 2.1$ on the near-IR emission from sample No. 5, but no convincing evidence for a corresponding signal at $g = 2$.

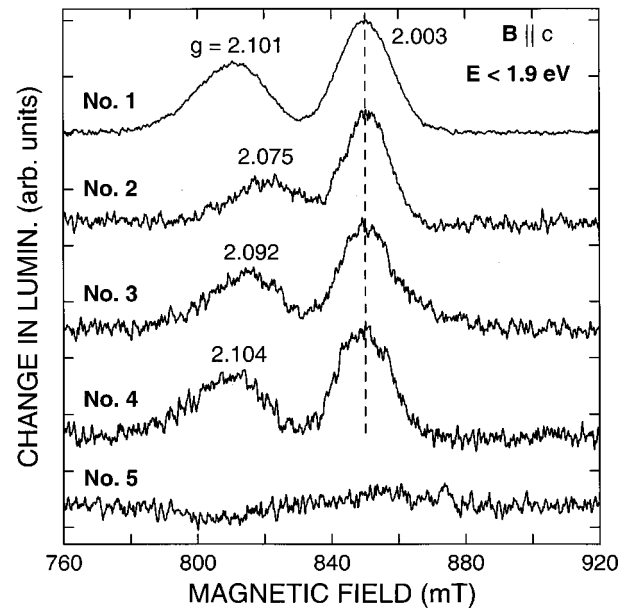
FIG. 6. g values of Mg-related ODMR signals at several PL energies for sample Nos. 1–3 with $\mathbf{B} \parallel c$.

IV. DISCUSSION

A. Defect assignments

1. Shallow Mg acceptors

Due to the absence of resolved hyperfine structure in most of the magnetic resonance reported to date for as-grown and

FIG. 7. ODMR spectra obtained on the near-IR emission from the five GaN:Mg samples with $\mathbf{B} \parallel c$. The feature with $g = 2.003$ is assigned to deep donors while the signal with $g \sim 2.1$ is ascribed to shallow Mg acceptors as described in the text.

doped GaN, including that described in this work, the microscopic identification of the various defect centers has been problematic. The donor or acceptor nature of the defects is typically made on the basis of whether the g values exhibit negative (donorlike) or positive (acceptorlike) shifts with respect to the free-electron g value of 2.0023. For example, there is strong consensus that the $g=1.95$ line observed in many EPR and ODMR studies during the last 8 years is associated with shallow donors or conduction electrons. This assignment is supported from EPR of GaN intentionally doped with Si (Ref. 28) and from $\mathbf{k}\cdot\mathbf{p}$ calculations of the Γ_7 conduction band g value.^{29,35}

We propose another strong case can now be made for the g values associated with SHALLOW Mg acceptors in GaN with $g_{\parallel}\sim 2.1$ and $g_{\perp}\sim 2.0$. This follows from the similarity of the EPR spin densities with the concentration of electronically active Mg acceptors determined by temperature-dependent Hall effect and the total [Mg] as revealed by SIMS. This assignment is further established by the observation of a similar resonance from ODMR on the recombination at 3.27(8) eV in sample Nos. 1 and 5. We note that the larger linewidths found for the Mg shallow acceptors in the ODMR experiments compared to those in the EPR arise mainly from the field-independent exchange interaction term (i.e., $J\mathbf{S}_D\cdot\mathbf{S}_A$, where J is a measure of the coupling strength between the donor and acceptor) that is often required to fully describe ODMR on donor-acceptor pair recombination. A similar resonance, also attributed to shallow Mg acceptors, was recently detected on the magnetic circular dichroism (MCD) of acceptor-bound excitons in CVD-grown GaN epitaxial layers with $[\text{Mg}]\sim 9\times 10^{18}\text{ cm}^{-3}$ (Ref. 36). In addition, magneto-PL studies have revealed a nearly isotropic g tensor for Mg acceptors involved in close pair SD-SA recombination in Mg-doped GaN homoepitaxial layers.³⁷

Although the g anisotropy for the shallow Mg acceptors (i.e., $\Delta g\equiv g_{\parallel}-g_{\perp}\sim 0.1$) is the largest reported to date for any acceptor in GaN, the degree of anisotropy is significantly smaller than expected (i.e., $g_{\parallel}\sim 2-4$, $g_{\perp}\sim 0$) from effective mass theory.^{38,39} An instructive parallel may be found in the properties of shallow acceptors in 4H- and 6H-SiC (Refs. 40 and 41) and CdS (Ref. 32), semiconductors with similar hexagonal symmetry, valence-band parameters, and shallow acceptor binding energies as found for GaN. For example, B, Al, and Ga have similar binding energies in 6H-SiC. However, B is Jahn-Teller distorted and has a nearly isotropic g tensor while Al and Ga are not distorted and have highly anisotropic g tensors. The nearly isotropic g tensor in the present case may reflect a symmetry-lowering local distortion of the Mg shallow acceptors.³⁸ This can arise, for example, from local fields associated with grain boundaries and/or that are generated from the size difference between the Mg atoms and the host Ga atoms they replace.⁴² The narrowing of the Mg shallow acceptor resonance observed for $\mathbf{B}\sim 30^\circ$ from the c axis in BOTH the EPR and ODMR experiments (see Figs. 3 and 4) possibly provides further evidence for such distortions. More work is needed to test this hypothesis, such as rotation studies in other crystallographic planes. We note that similar narrowing behavior was not observed for the magnetic resonance of shallow accep-

tors with highly anisotropic g tensors in 4H- and 6H-SiC and CdS.

Based on the similarity with the EPR results and the ODMR on the 3.27–3.28 eV SD-SA PL bands, including nearly identical g tensors and linewidth behavior with field orientation, the broad ODMR resonances observed on the 2.8–3.2 eV PL bands and on the emission less than 1.9 eV are also assigned to shallow Mg acceptors. For the broad “blue” PL bands, it was suggested previously⁴ that the shift in g values towards 2 and the decrease in anisotropy from 0.135 to 0.044 could be interpreted as a deepening of the binding energy for the Mg-related centers. However, in light of the small variation also observed in the Mg EPR g tensors ($\Delta g=0.073-0.113$) and the energy-dependent ODMR g values (see Fig. 6), we propose that other factors are likely responsible for this variation. The similarity of g_{\parallel} values found for the acceptor resonances in the low- and high-Mg-doped sample Nos. 1 and 5, respectively, suggests that effects due to Mg concentration alone cannot account for the small changes in g values among these samples and that reported previously for Mg doping levels up to $5\times 10^{19}\text{ cm}^{-3}$ (Refs. 33, 36, 43, and 44). One possible source of additional distortions at the Mg sites (resulting in further reductions of the g anisotropy from that found on the 3.27-eV PL band) are electric fields associated with large potential fluctuations that have been proposed to play a role in recombination from highly doped and compensated GaN. More work is required to account more definitively for the small changes in the resonance parameters of these Mg-related centers.

We note that recent EPR experiments⁴⁵ on GaN layers with $[\text{Mg}]\sim 10^{20}\text{ cm}^{-3}$ and codoped with Si between $1-5\times 10^{18}\text{ cm}^{-3}$ (i.e., much higher than the typical residual levels of Si and O as determined by SIMS) revealed signals with $g_{\parallel}\sim 2.070$ and $g_{\perp}\sim 2.057$ and spin densities of $\sim 2\times 10^{19}\text{ cm}^{-3}$. Most notably, the g anisotropies of ~ 0.013 are MUCH smaller than those obtained for sample Nos. 3–5 with $[\text{Mg}]\leq 5\times 10^{19}\text{ cm}^{-3}$. This result combined with the low room-temperature hole concentrations ($\sim 1-5\times 10^{16}\text{ cm}^{-3}$) found from Hall effect suggests an assignment of this line to Mg-related or -induced deep centers (probably acceptorlike based on the g values). Alternatively, it cannot be excluded that this feature is associated with severely perturbed shallow Mg acceptors and that the reduced p -type conduction reflects a high level of compensating donors (possibly Mg related) introduced under these doping conditions. We note that the transport properties of these films contrast with predictions of enhanced room-temperature hole densities via this codoping technique.⁴⁶

2. Shallow and deep donors

As noted earlier, the $g=1.95$ line observed on the 3.27–3.28 eV SD-SA PL from sample Nos. 1 and 5 is regarded as a “fingerprint” for shallow donors and conduction electrons in GaN. Based on the small difference (~ 0.01) with this g value, we propose that the resonance with $g\sim 1.96$ observed on the broad 2.8–3.2 eV PL bands from sample Nos. 2–4 is also likely associated with shallow donors. The small shift in g values toward $g=2$ and the broadening can be understood

by an increase in the exchange interaction³ due to the reduced average donor-acceptor pair separation in these more heavily doped samples. Similar g shifts and broadening behavior were recently demonstrated from microwave modulation frequency studies of the ODMR on the 3.2 eV PL band from sample No. 2 (Ref. 4).

Though we believe it is unlikely, in the absence of more detailed magnetic resonance information such as provided by resolved hyperfine interaction, the association of the $g \sim 1.96$ line with deep donors can not be excluded at this time. However, combined with the near-midgap PL energy and the observation of shallow Mg acceptors (see Fig. 7), the strongest evidence from this work for the existence of deep donors is the isotropic $g = 2.003$ resonance on the emission less than 1.9 eV. We note that these centers are described by a different g tensor than that for the deep defects [i.e., $g_{\parallel} = 1.989(1)$ and $g_{\perp} = 1.992(1)$] found on the 2.2-eV “yellow” luminescence band from GaN (Ref. 33).

B. Recombination models

1. 2.8–3.2 eV “blue” PL bands

Much attention has been given lately to the origin of the broad 2.8–3.2 eV emission bands from heavily Mg-doped GaN as observed for sample Nos. 2–4. As mentioned earlier, the 3.2-eV PL band as observed from sample No. 2 has been attributed to recombination between shallow donors and shallow acceptors in the presence of large potential fluctuations.⁵ In contrast to that work for samples with similar Mg doping levels, the emission from sample No. 2 retains a structureless, broad character with increasing excitation power density (we note that similar PL behavior was observed by another group²² for a particular highly N-doped and compensated ZnSe sample). Thus it is difficult to draw conclusions from the low-temperature (cw) PL study alone on the shallow and deep character of the donors and acceptors that participate in this recombination. However, based on the interpretations of the g tensors given above, the ODMR suggests a shallow character for both the donor and (Mg) acceptor centers involved in this emission. In addition, from a simple picture with shallow donor and acceptor Bohr radii of ~ 25 and 5 \AA , respectively, the strong ODMR observed in this sample is surprising (for these microwave powers) based on the fast lifetimes (< 100 ns) expected from an estimate of the average donor-acceptor pair separation of $\sim 15 \text{ \AA}$. Thus, though not evident from the PL power study, the strength of the ODMR signals can be understood from the presence of potential fluctuations that lead to additional separation of the shallow donors and acceptors under the low photoexcitation conditions employed in this work.

Two models are considered to account for the broad 2.8-eV PL bands (see Fig. 8) observed from more highly Mg-doped sample Nos. 3 and 4 based on these magnetic resonance studies. Two key aspects are noted. First, in both schemes, one of the recombination partners is attributed to shallow Mg acceptors. Second, as argued in Sec. IV A 2, the $g = 1.96$ ODMR feature (SIMILAR to that observed on the broad 3.2 eV band) is ascribed to shallow rather than deep donors. As used to describe the 3.2 eV PL, the 2.8 eV PL in

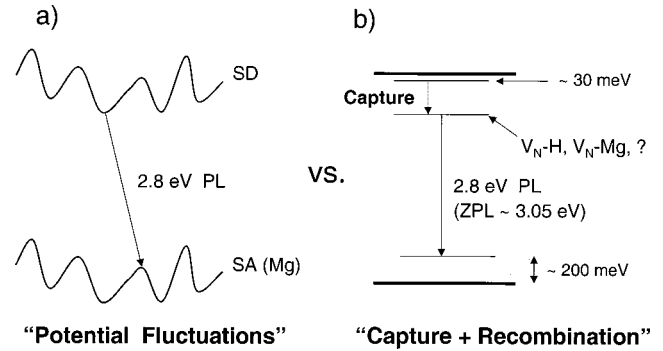


FIG. 8. Possible recombination models for the broad 2.8-eV PL band typically observed in CVD-grown GaN with $[\text{Mg}] \geq 2 \times 10^{19} \text{ cm}^{-3}$. (a) Recombination between shallow donors and shallow Mg acceptors in the presence of large potential fluctuations. (b) Two-step process involving spin-dependent capture followed by radiative recombination between deep donors and shallow Mg acceptors. The estimate for the zero-phonon line of ~ 3.05 eV is taken from Ref. 6.

the first model [Fig. 8(a)] is attributed to radiative recombination between these shallow donors and shallow Mg acceptors in the presence of large potential fluctuations. In this scheme, the additional redshift of this band relative to the broad 3.2 eV PL is explained by an increase in magnitude of the potential fluctuations. This can arise from a higher degree of donor compensation (hence higher donor concentrations) with increasing Mg doping as observed by others.¹⁴ Both charged shallow and deep donors can contribute to these fluctuations. Most notably, the sum of the residual Si and O shallow donor concentrations for sample Nos. 3 and 4 (see Table II) cannot account for all of the compensating donors ($\sim 2 \times 10^{18} \text{ cm}^{-3}$) as revealed by the temperature-dependent Hall effect measurements. Hence this suggests the presence of other donors (possibly induced by Mg doping) of shallow and/or deep character. As discussed above, we suggest that ODMR on the 2.8-eV PL bands only reveals evidence for shallow donors while the existence of deep donors in these samples is indeed found from ODMR on the broad emission less than 1.9 eV.

Several groups have argued^{5–12} that the 2.8-eV PL band arises from recombination between deep donors (possibly Mg related) and shallow Mg acceptors. This has been proposed, for example, from the behavior of the emission under large hydrostatic pressures¹¹ and similarly suggested from a self-compensation model employed to describe the dependence of the hole concentration as a function of the Mg doping level.¹² In order to be consistent with this model, a more complicated ODMR mechanism must be invoked such as shown, for example, in Fig. 8(b). Similar to the model proposed for the 2.2-eV “yellow” luminescence band several years ago,³³ the ODMR occurs via spin-dependent capture of an electron from the EM donor state ($E_d \sim 30 \text{ meV}$) to these deep donors. This is followed by radiative recombination between the deep donors and shallow Mg acceptors ($E_a \sim 200 \text{ meV}$). It is puzzling, however, that such deep donors could not be directly observed from the ODMR in this work and that reported by others^{36,43,44} on similar PL. We note that

time-resolved PL measurements have revealed nonexponential time decays with nominal lifetimes of $\sim 1 \mu\text{s}$ for the 2.8-eV “blue” PL band in similar Mg-doped GaN layers.^{47,48} Such behavior can support either of the models given in Fig. 8. Other recombination mechanisms cannot be excluded at this time.

2. $PL < 1.9 \text{ eV}$

The ODMR on the emission less than 1.9 eV from sample Nos. 1–4 strongly suggests that the transition involves deep donors (possibly Mg related or induced) and shallow Mg acceptors. This assignment differs from the deep donor to deep acceptor model proposed by another group⁶ to account for similar emission in GaN doped with Si and Mg. We note that the absence of the deep donors with $g = 2.003$ (see Fig. 7) and the observation of SD-SA recombination at 3.28 eV rather than the broad 2.8-eV PL band for HIGHLY Mg-doped (*p*-type) sample No. 5 suggest the important roles these centers may play in both the optical and transport properties of Mg-doped GaN.

V. SUMMARY

EPR and ODMR experiments have been performed on several GaN epitaxial layers doped with Mg from 2.5×10^{18} to $5.0 \times 10^{19} \text{ cm}^{-3}$ to address factors such as self-compensation, complexing, etc., that are suggested to partially limit typical room-temperature hole densities in the range of $1 - 5 \times 10^{17} \text{ cm}^{-3}$. In addition, an attempt was made to correlate the results with those from SIMS, temperature-dependent Hall effect, and low-temperature PL in order to form a self-consistent picture and, thus, improve the current

understanding of this interesting and technologically important doping problem.

A single EPR feature with $g_{\parallel} \sim 2.1$ and $g_{\perp} \sim 2$ was found for three samples with room-temperature hole densities between 9×10^{16} and $2 \times 10^{17} \text{ cm}^{-3}$. This line is assigned to shallow Mg acceptors from a comparison of the spin densities with the number of electrically active Mg centers determined from analyses of the Hall effect and the total Mg given by SIMS. ODMR on the shallow-donor–shallow-acceptor PL at 3.27 eV and on the broad 2.8–3.2 eV emission bands revealed two resonance features attributed to shallow donors with $g \sim 1.95 - 1.96$ and to shallow Mg acceptors based on the similarity of the g tensors with those found by EPR. Though puzzling in light of recent reports, no clear evidence was found for deep donors from ODMR on the 2.8-eV “blue” emission band. However, in addition to shallow Mg acceptors, evidence for deep donors with isotropic g values of 2.003 was found on broad emission less than 1.9 eV from several of the samples. More work is needed to make a definitive chemical identification of these deep donors such as might be provided by optically detected electron-nuclear double-resonance (ODENDOR) experiments.

ACKNOWLEDGMENTS

We would like to thank T. A. Kennedy (NRL), R. Kotlyar, A. L. Efros (NRL), and I. A. Merkulov (Ioffe Institute) for many helpful discussions. Thanks are also due S. C. Binari (NRL) and R. J. Gorman (NRL) for electrical transport measurements of some of the samples investigated in these studies. This work was supported by the Office of Naval Research.

*Permanent address: Physics Institute, Universidade de Brasilia, Brasilia, Brazil.

†Current address: SFA Inc., Largo, MD 20744.

‡Current address: Army Research Laboratory, Adelphi, MD 20783-1197.

§Current address: Sandia National Laboratory, Albuquerque, NM 87185.

||Current address: Cree Lighting Company, Goleta, CA 93117.

¹See, e.g., D. P. Bour, H. F. Chung, W. Götz, L. Romano, B. S. Krusor, D. Hofstetter, S. Rudaz, C. P. Kuo, F. A. Ponce, N. M. Johnson, M. G. Craford, and R. D. Bringans, in *III-V Nitrides*, edited by F. A. Ponce, T. D. Moustakes, I. Akasaki, and B. A. Monemar, Mater. Res. Soc. Symp. Proc. No. **449** (Materials Research Society, Pittsburgh, 1997), p. 507.

²See, for example, E. Calleja, M. A. Sánchez-García, F. Calle, F. B. Naranjo, E. Muñoz, U. Kahn, K. Ploog, J. Sánchez, J. M. Calleja, K. Saarinen, J. Oila, and P. Hautojärvi, Mater. Sci. Eng., B **82**, 2 (2001), and references therein.

³For a review, see T. A. Kennedy and E. R. Glaser, in *Identification of Defects in Semiconductors*, Semiconductors and Semimetals Vol. 51A, edited by M. Stavola (Academic, San Diego, 1998), pp. 93–136.

⁴E. R. Glaser, T. A. Kennedy, J. A. Freitas, Jr., B. V. Shanabrook, A. E. Wickenden, D. D. Koleske, R. L. Henry, and H. Obloh, Physica B **273–274**, 58 (1999).

⁵M. A. Reshchikov, G. C. Yi, and B. W. Wessels, Phys. Rev. B **59**, 13 176 (1999).

⁶U. Kaufmann, M. Kunzer, H. Obloh, M. Maier, Ch. Manz, A. Ramakrishnan, and B. Santic, Phys. Rev. B **59**, 5561 (1999).

⁷S. G. Lee and K. J. Chang, Semicond. Sci. Technol. **14**, 138 (1999).

⁸L. Eckey, U. von Gfug, J. Holst, A. Hoffmann, A. Kaschner, H. Siegle, C. Thomsen, B. Schineller, K. Heime, M. Heuken, O. Schöen, and R. Beccard, J. Appl. Phys. **84**, 5828 (1998).

⁹P. H. Lim, B. Schineler, O. Schöen, K. Heime, and M. Heuken, J. Cryst. Growth **205**, 1 (1999).

¹⁰F. Shahedipour and B. W. Wessels, Appl. Phys. Lett. **76**, 3011 (2000).

¹¹H. Teisseyre, T. Suski, P. Perlin, I. Grzegory, M. Leszczynski, M. Bockowski, S. Porowski, J. A. Freitas, Jr., R. L. Henry, A. E. Wickenden, and D. D. Koleske, Phys. Rev. B **62**, 10 151 (2000).

¹²U. Kaufmann, P. Schlotter, H. Obloh, K. Köhler, and M. Maier, Phys. Rev. B **62**, 10 867 (2000).

¹³A. E. Wickenden, D. K. Gaskill, D. D. Koleske, K. Doverspike, D. S. Simons, and P. H. Chi, in *Gallium Nitride and Related Materials*, edited by R. D. Dupuis, J. A. Edmond, F. A. Ponce, and S. Nakamura, Mater. Res. Soc. Symp. Proc. No. **395** (Materials Research Society, Pittsburgh, 1996), p. 679.

¹⁴P. Kozodoy, H. Xing, S. P. DenBaars, U. K. Mishra, A. Saxler, R. Perrin, S. Elhamri, and W. C. Mitchel, J. Appl. Phys. **87**, 1832 (2000).

- ¹⁵We note that the Si, O, C, and H concentrations are all above the SIMS detectivity limits given by Charles Evans and Associates.
- ¹⁶M. Ilegems and R. Dingle, *J. Appl. Phys.* **44**, 4234 (1973).
- ¹⁷H. Amano, M. Kitoh, K. Hiramatsu, and I. Akasaki, *J. Electrochem. Soc.* **137**, 1639 (1990).
- ¹⁸J. A. Freitas, Jr., T. A. Kennedy, E. R. Glaser, and W. E. Carlos, *Solid-State Electron.* **41**, 185 (1997).
- ¹⁹G. C. B. Braga, J. A. Freitas, Jr., and P. B. Klein (unpublished).
- ²⁰W. J. Moore, J. A. Freitas, Jr., G. C. B. Braga, R. J. Molnar, S. K. Lee, K. Y. Lee, and I. J. Song, *Appl. Phys. Lett.* **79**, 2570 (2001).
- ²¹H. P. Gislason, B. H. Yang, and M. Linnarson, *Phys. Rev. B* **47**, 9418 (1993).
- ²²P. Bäüme, J. Gutowski, D. Wiesmann, R. Heitz, A. Hoffmann, E. Kurtz, D. Hommel, and G. Landwehr, *Appl. Phys. Lett.* **67**, 1914 (1995).
- ²³I. Kuskovsky, D. Li, G. F. Neumark, V. N. Bondarev, and P. V. Pikhitsa, *Appl. Phys. Lett.* **75**, 1243 (1999).
- ²⁴B. I. Shklovskii and A. L. Efros, *Electronic Properties of Doped Semiconductors* (Springer, Berlin, 1984).
- ²⁵M. Kunzer and U. Kaufmann (private communication).
- ²⁶See, for example, E. E. Reuter, R. Zhang, T. F. Kuech, and S. G. Bishop, *MRS Internet J. Nitride Semicond. Res.* **4S1**, G3.67 (1999).
- ²⁷M. W. Bayerl, M. S. Brandt, E. R. Glaser, A. E. Wickenden, D. D. Koleske, R. L. Henry, and M. Stutzmann, *Phys. Status Solidi B* **216**, 547 (1999).
- ²⁸M. W. Bayerl, M. S. Brandt, O. Ambacher, M. Stutzmann, E. R. Glaser, R. L. Henry, A. E. Wickenden, D. D. Koleske, T. Suski, I. Grzegory, and S. Porowski, *Phys. Rev. B* **63**, 125203 (2001).
- ²⁹M. Palczewska, B. Suchanek, R. Dwilinski, K. Pakula, A. Wagner, and M. Kaminska, *MRS Internet J. Nitride Semicond. Res.* **3**, 45 (1998).
- ³⁰W. E. Carlos, J. A. Freitas, Jr., M. Asif Khan, D. T. Olson, and J. N. Kuznia, *Phys. Rev. B* **48**, 17 878 (1993), and references therein.
- ³¹N. M. Reinacher, H. Angerer, O. Ambacher, M. S. Brandt, and M. Stutzmann, in *III-V Nitrides*, (Ref. 1), p. 579.
- ³²See, for example, J. L. Patel, J. E. Nicholls, and J. J. Davies, *J. Phys. C* **14**, 139 (1981).
- ³³E. R. Glaser, T. A. Kennedy, K. Doverspike, L. B. Rowland, D. K. Gaskill, J. A. Freitas, Jr., M. Asif Khan, D. T. Olson, J. N. Kuznia, and D. K. Wickenden, *Phys. Rev. B* **51**, 13 326 (1995).
- ³⁴C. Bozdog, H. Przbylinska, G. D. Watkins, V. Härle, F. Scholz, M. Mayer, M. Kamp, R. J. Molnar, A. E. Wickenden, D. D. Koleske, and R. L. Henry, *Phys. Rev. B* **59**, 12 479 (1999).
- ³⁵M. W. Bayerl, M. S. Brandt, T. Graf, O. Ambacher, J. A. Majewski, and M. Stutzmann, *Phys. Rev. B* **63**, 165204 (2001).
- ³⁶D. M. Hofmann, W. Burkhardt, F. Leiter, W. von Forster, H. Alves, A. Hofstaetter, B. K. Meyer, N. Romanov, H. Amano, and I. Akasaki, *Physica B* **273–274**, 43 (1999).
- ³⁷R. Stepniewski, A. Wyszomolek, M. Potemski, J. Lusakowski, K. Korona, K. Pakula, J. M. Baranowski, G. Martinez, P. Wyder, I. Grzegory, and S. Porowski, *Phys. Status Solidi B* **210**, 373 (1998).
- ³⁸A. V. Malyshev, I. A. Merkulov, and A. V. Rodina, *Phys. Solid State* **40**, 917 (1998).
- ³⁹R. Kotlyar (private communication).
- ⁴⁰Le Si Dang, K. M. Lee, G. D. Watkins, and W. J. Choyke, *Phys. Rev. Lett.* **45**, 390 (1980).
- ⁴¹P. G. Baranov, *Defect Diffus. Forum* **148–149**, 129 (1997), and references therein.
- ⁴²T. N. Morgan, in *Proceedings of the Tenth International Conference on the Physics of Semiconductors*, edited by S. P. Keller, J. C. Hensel, and F. Stern (U.S. AEC Division of Technical Information, Springfield, VA, 1970), p. 266.
- ⁴³U. Kaufmann, M. Kunzer, C. Merz, I. Akasaki, and H. Amano, in *Gallium Nitride and Related Materials* (Ref. 13), p. 633, and references therein.
- ⁴⁴F. K. Koschnick, K. Michael, J.-M. Spaeth, B. Beaumont, P. Gibart, J. Off, A. Sohmer, and F. Scholz, *J. Cryst. Growth* **189–190**, 561 (1998).
- ⁴⁵W. E. Carlos, R. L. Henry, A. E. Wickenden, and D. D. Koleske (unpublished).
- ⁴⁶H. Katayama-Yoshida and T. Yamamoto, *J. Cryst. Growth* **189/190**, 532 (1998).
- ⁴⁷Y.-H. Kwon, S. K. Shee, G. H. Gainer, G. H. Park, S. J. Hwang, and J. J. Song, *Appl. Phys. Lett.* **76**, 840 (2000).
- ⁴⁸F. Shahedipour and B. W. Wessels, *MRS Internet J. Nitride Semicond. Res.* **6**, 12 (2001).